CHEMPHYSCHEM

DOI: 10.1002/cphc.200800544

Temperature and Concentration Effects on the Solvophobic Solvation of Methane in Aqueous Salt Solutions

Jörg Holzmann,[a] Ralf Ludwig,*[a, b] Alfons Geiger,[c] and Dietmar Paschek[c, d]

We perform molecular dynamics (MD) simulations of aqueous salt (NaCl) solutions using the TIP4P-Ew water model (Horn et al., J. Chem. Phys. ***2004****,* 120*, 9665) covering broad temperature and concentration ranges extending deeply into the supercooled region. In particular we study the effect of temperature and salt concentration on the solvation of methane at infinite dilution. The salt effect on methane's solvation free energy, solvation enthalpy and entropy, as well as their temperature dependence is found to be semi-quantitatively in accordance with the data of Ben-Naim and Yaacobi (*J. Phys. Chem. ***1974****,* 78*, 170). To distinguish the influence of local (in close proximity to ions) and global effects, we partition the salt solutions into ion influenced hydration shell regions and bulk water. The chemical potential of methane is systematically affected by the presence of salt in both sub volumes, emphasizing the importance of the global volume contraction due to electrostriction effects. This observation is correlated with systematic structural alterations similar to water under pressure. The observed electrostriction effects are found to become increasingly pronounced under cold (supercooled) conditions. We find that the influence of temperature and salt induced global density changes on the solvation properties of methane is well recovered by simple scaling relation based on predictions of the information theory model of Garde et al. (*Phys. Rev. Let. ***1999****,* 77*, 4966).*

1. Introduction

Nonpolar small solutes, such as noble gases or alkanes, don't like to be dissolved in water: They are "hydrophobic". Their corresponding solvation free energy is found to be large and positive and is caused by a dominating negative solvation entropy, which has been related to the specific structural peculiarities of the hydrophobic hydration shell.[1–4] Adding salt (NaCl) significantly decreases the solubility and therefore increases the solvation free energy, but is at the same time found to reduce the solvation entropy.[5] The increasing excess chemical potential, but also the effect on the entropy, is found to scale monotonously with the salt concentration. The corresponding "salting out" tendency can be excellently described by Setschenow's empirical concentration independent coefficient.[6,7] It is, however, still a matter of debate how exactly the solvation properties are affected by the ions.[8]

Essentially two different scenarios have been put forward to explain salt effects in general. Firstly, it has been suggested that a modification of the water structure is the origin[9] of the solvation changes. It has been hypothesized that some ions ("kosmotropes") enhance the water structure surrounding the ions which leads to a strengthening of the hydrophobic effect and thereby for example, stabilize the proteins.[10] On the other hand, the ions which break the structure surrounding the ions ("chaotropes") have been considered to weaken the hydrophobic effect, and hence destabilize the native state of proteins. It has been suggested that the competition between ionic charge and ionic size determines whether an ion is a chaotrope or a kosmotrope.[11–15] Sodium chloride is considered as a weak kosmotrope.[16] Recently Thomas and Elcock reported a good linear correlation between experimental Setchenow "salting-out" coefficients and the extent of water–water hydrogen bonding computed from simulations.[17] A completely different explanation has been suggested by Timasheff and co-workers.[18,19] They consider the difference in salt-binding as the main effect. Their analysis of thermodynamic data of salt effects on protein stability provide evidence that the salts which denature proteins tend to be bound to proteins, whereas the salts which stabilize proteins tend to be excluded from the protein surface. A recent simulation study by Zangi, Hagen and Berne[20] could indeed show that the ion-adsorption mechanism could explain the association-behavior of idealized hydrophobic plates. Moreover, a recent study by Athawale, Sarupria and Garde[21] showed that hydrophobic solvation acts differently on small and large length-scales, concerning solute size and distance.

[a] *J. Holzmann, Prof. Dr. R. Ludwig*
Institut für Chemie, Abteilung Physikalische Chemie
Universität Rostock, Dr.-Lorenz-Weg 1,D-18051 Rostock (Germany)
Fax: (+49) 381-498-6524
E-mail: ralf.ludwig@uni-rostock.de

[b] *Prof. Dr. R. Ludwig*
Leibniz Institut für Katalyse an der Universität Rostock
Albert-Einstein-Str. 29a,D-18059 Rostock (Germany)

[c] *Prof. Dr. A. Geiger, Dr. D. Paschek*
Physikalische Chemie, Fakultät Chemie, TU Dortmund
Otto-Hahn-Str. 6,D-44227 Dortmund (Germany)

[d] *Dr. D. Paschek*
Lehrstuhl Thermodynamik, Fakultät Bio- und Chemieingenieurwesen
TU Dortmund, Emil-Figge-Str. 70,D-44227 Dortmund (Germany)

Supporting Information for this article is available on the WWW under http://dx.doi.org/10.1002/cphc.200800544.

Herein we discuss the balance of local (ion adsorption) and global (structural alterations) effect on the "salting out" behavior of perhaps the most simple small apolar solute: methane. Numerous studies have addressed the solvation of methane.[21–26] Here we focus on the determination of thermodynamic solvation properties of methane in a TIP4P-Ew model solvent and demonstrate that the simulations semi-quantitatively reproduce the thermodynamic signatures of the salt effect upon the solvophobic solvation of methane over large temperature and concentration ranges. To be able to separate local (close to ions) and global effects, we partition the salt solutions into ion influenced hydration shell regions and bulk water, as applied recently.[27] In addition, we monitor the structural and volume changes of the solvent under changing salt concentration and temperature conditions. This is motivated by the recent observation that density changes and changing solvation properties are tightly related.[28,29]

Methods

MD Simulations

We present molecular-dynamics simulations of aqueous salt solutions using system sizes of 1000 TIP4P-Ew model water molecules[30] plus additional NaCl ion pairs. Sodium chloride potential parameters reported by Heinzinger[31] were employed ($\sigma_{Na}=0.273$ nm, $\varepsilon_{Na}k_B^{-1}=43.06$ K, $\sigma_{Cl}=0.486$ nm, $\varepsilon_{Cl}k_B^{-1}=20.21$ K). Standard Lorentz-Berthelot mixing rules were applied to determine Lennard–Jones cross interactions. The electrostatic interactions are treated in the "full potential" approach by the smooth particle mesh Ewald summation[32] with a real space cutoff of 0.9 nm and a mesh spacing of approximately 0.12 nm and 4th order interpolation. The Ewald convergence factor α was set to 3.38 nm^{-1} (corresponding to a relative accuracy of the Ewald sum of 10^{-5}). A 2.0 fs timestep was used for all simulations and the geometric constraints were solved using the SETTLE procedure.[33] All simulations were carried out by the GROMACS 3.2 simulation program.[34] The simulations were performed under isobaric/isothermal conditions for a pressure of 1 bar using a Nosé–Hoover[35,36] thermostat and a Rahman–Parrinello barostat[37,38] with coupling times of $\tau_T=1.0$ ps, and $\tau_P=2.0$ ps (assuming the isothermal compressibility to be $\chi_T=4.5\times10^{-5}$ bar^{-1}). All properties were studied for the temperature range between 230 and 400 K for varying salt concentrations (all investigated statepoints are collected in Table 1). In addition also simulations of the pure solvent (1000 TIP4P-Ew) were performed. Each of the in total 144 simulation runs was at least 12 ns long.

Solvation Properties of Methane

The solvation free energy per methane particle is given by the excess chemical potential μ_{ex}. We determined μ_{ex} for the case of infinite dilution *a posteriori* from the MD-trajectories applying Widom's potential distribution theorem[39] with $\mu_{ex}=-kT\ln\{\langle V\exp[-\beta\Phi(\vec{r})]\rangle/\langle V\rangle\}$. Here is $\beta=1/kT$, V the volume of the simulation box, and $\Phi(\vec{r})$ is the potential energy of a randomly inserted (gas) test-particle at position $\vec{r}$. The brackets $\langle\ldots\rangle$ indicate isobaric isothermal sampling as well as sampling over many different positions $\vec{r}$. The interaction parameters according to Hirschfelder et al. for methane were used ($\sigma=3.730$ nm and $\varepsilon/k=147.5$ K).[40,41] To determine the methane solvent cross parameters the Lorentz–Berthelot mixing rules were applied. We have validated the accuracy of the estimated solvation free energies by independent calculations employing overlapping distribution functions.[42,43] These data are provided in the Supporting Information.

Table 1. Sodium chloride concentrations (given in $mol\,l^{-1}$) as obtained from the MD simulations as a function of temperature for the different compositions (given in mol% NaCl in the first row). Each simulation consisted of 1000 TIP4P-Ew water molecules and 5, 10, 15, 20, 30, 40 , and 50 ion pairs, respectively.

T [K]	0.49	0.99	1.48	1.96	2.91	3.85	4.76
230	0.272	0.542	0.809	1.073	1.589	2.091	2.575
240	0.274	0.545	0.813	1.077	1.593	2.092	2.573
250	0.275	0.547	0.815	1.079	1.594	2.092	2.572
260	0.276	0.548	0.816	1.080	1.593	2.090	2.568
270	0.276	0.548	0.815	1.078	1.591	2.085	2.561
280	0.276	0.547	0.814	1.076	1.587	2.079	2.553
290	0.275	0.546	0.812	1.073	1.581	2.071	2.543
300	0.274	0.544	0.809	1.069	1.575	2.063	2.532
310	0.273	0.542	0.805	1.064	1.568	2.052	2.519
320	0.272	0.539	0.801	1.059	1.560	2.041	2.506
330	0.270	0.536	0.796	1.052	1.550	2.030	2.491
340	0.268	0.532	0.791	1.046	1.541	2.017	2.475
350	0.267	0.529	0.786	1.039	1.530	2.003	2.459
360	0.264	0.524	0.780	1.031	1.519	1.989	2.441
370	0.262	0.520	0.774	1.023	1.507	1.974	2.423
380	0.260	0.516	0.767	1.014	1.495	1.958	2.404
390	0.258	0.511	0.760	1.005	1.482	1.941	2.384
400	0.255	0.506	0.753	0.996	1.468	1.924	2.363

The entropic and enthalpic contributions to the excess chemical potential are obtained as temperature derivatives according to $s_{ex}=-[\partial\mu_{ex}/\partial T]_P$ and $h_{ex}=-T^2[\partial(\mu_{ex}/T)/\partial T]_P$. The corresponding heat capacity of solvation is available as second derivative $C_{Pex}=-T[\partial^2\mu_{ex}/\partial T^2]_P$.

In addition, we also determine the methane–solvent pair distribution functions $g(r)$ by calculating the corresponding profiles of free energy $w(r)$, that is, we employ the potential distribution theorem[39] with $w(r)=-kT\ln\{\langle V\exp(-\beta\Phi(\vec{r}_1)\delta(|\vec{r}_1-\vec{r}_2|-r)\rangle/\langle V\rangle\}-\mu_{ex}$. Here $\Phi(\vec{r}_1)$ is the energy of randomly inserting the gas particle and $\vec{r}_2$ refers to the position of the reference (solvent) site within the simulation box. μ_{ex} is the excess chemical potential of a single gas particle. The profile of free energy $w(r)$ is related to the corresponding radial pair distribution function $g(r)$ according to $-kT\ln g(r)=w(r)$.[2,39] Similar to the computation of μ_{ex}, $w(r)$ has been calculated *a posteriori* from stored trajectory data using exactly the same Monte Carlo sampling procedure.

In order to improve the computational efficiency, we have made use of the excluded volume map (EVM) technique[44,45] by mapping the occupied volume onto a grid of approximately 0.2 Å meshwidth. Distances smaller than $0.7\times\sigma_{ij}$ with respect to any solute molecule were neglected and the term $\exp(-\beta\Phi)$ taken to be zero. This simple scheme improves the efficiency of the sampling by almost two orders of magnitude. For the calculation of the (Lennard–Jones) insertion energies Φ we have used cut-off distances of 10 Å in combination with a proper cut-off correction. Each configuration has been probed by 2×10^3 successful insertions (i.e. insertions into the free volume contributing non-vanishing Boltzmann-factors). About 2.4×10^4 configurations were analyzed per state point.

2. Results and Discussion

2.1. Salt Effect on the Solvation Free Energy and its Temperature Derivatives

The excess chemical potentials for methane μ_{ex} as a function of temperature for various salt concentrations are shown in Figures 1 and 2 and are given in Table 2. Derivatives of the solvation free energy with respect to temperature, as well as free energy data for temperatures other than listed in Table 2 were calculated from fitted third-order polynomials.[46] The experimental data of the solvation of methane in pure water and aqueous salt solutions shown in Figures 1 and 2 have been directly calculated from the Ostwald coefficients $\gamma = \exp[-\mu_{ex}/kT]$ given by Ben–Naim and Yaacobi.[5] To determine the excess chemical potentials (solvation free energies) and thermodynamic derivatives, we have used their tabulated polynomial coefficients for γ.

Table 2. Excess chemical potentials μ_{ex} (given in kJ mol^{-1}) of methane dissolved in aqueous sodium chloride solutions of different concentrations (given in mol% NaCl in the first row) as a function of temperature. The accuracy $\delta\mu_{ex}$ has been estimated to vary from about ± 0.05 kJ mol^{-1} for the highest temperature to about ± 0.2 kJ mol^{-1} at 230 K.

T [K]	0.0	0.49	0.99	1.48	1.96	2.91	3.85	4.76
230	3.79	4.21	4.57	5.01	5.40	5.82	6.48	7.22
240	4.92	5.32	5.53	5.98	6.24	6.90	7.54	8.20
250	5.82	6.26	6.51	6.82	7.18	7.94	8.45	9.18
260	6.63	6.97	7.45	7.64	8.02	8.65	9.20	9.82
270	7.50	7.79	8.22	8.49	8.80	9.41	9.95	10.51
280	8.24	8.57	8.94	9.22	9.47	10.03	10.66	11.21
290	8.91	9.27	9.55	9.80	10.17	10.73	11.07	11.79
300	9.48	9.82	10.12	10.40	10.68	11.19	11.73	12.20
310	10.06	10.37	10.61	10.86	11.20	11.72	12.22	12.69
320	10.46	10.77	11.11	11.34	11.68	12.17	12.64	13.17
330	10.90	11.23	11.51	11.79	12.06	12.54	13.02	13.52
340	11.27	11.54	11.83	12.15	12.43	12.89	13.36	13.84
350	11.58	11.90	12.17	12.44	12.70	13.19	13.63	14.13
360	11.81	12.14	12.38	12.71	12.92	13.42	13.91	14.38
370	12.04	12.31	12.66	12.88	13.16	13.64	14.14	14.54
380	12.17	12.50	12.79	13.08	13.33	13.81	14.27	14.70
390	12.34	12.63	12.91	13.20	13.46	13.91	14.41	14.86
400	12.40	12.75	13.02	13.29	13.57	14.03	14.49	14.93

The obtained value for the excess chemical potential of methane in pure water at 300 K of 9.48 kJ mol^{-1} is similar to the value reported by Krouskop,[47] and is reasonably close to the simulated values of 9.79 kJ mol^{-1} and 9.78 kJ mol^{-1} obtained by Shimizu and Chan, as well as Paschek[28,48,49] for the TIP4P model at 298 K and 300 K and 1 atm, respectively. However, the value is about 1 kJ mol larger than the experimental value of 8.4 kJ mol^{-1}.[5] Dyer et al. have recently shown that this difference can be significantly reduced when the solute polarizability is explicitly considered.[50] The polarizability has been shown to introduce a largely temperature and density insensitive offset to the chemical potential and therefore affects only mildly the derivatives of the free energy.[28] Docherty et al. used a specifically modified combination rule for methane-water interactions to effectively capture this effect and improve the solvation free energies.[25] Despite these efforts, we have preferred to take the original parameters of Hirschfelder[40] facing the fact that the hydrophobic hydration of Lennard–Jones solutes in a limited parameter range behave very similarly on a qualitative to semi-quantitative level.[28]

Figure 1 reveals that the temperature dependence of the simulated excess chemical potentials, as well as the derived enthalpic and entropic contributions behave qualitatively compatible to the experimental data reported by Ben-Naim and Yaacobi.[5] The excess chemical potentials of methane in water and the aqueous solution is positive and increases with temperature, being consistent with a dominating negative entropy of hydrophobic solvation. However, both the solvation enthalpy h_{ex} and the contribution from the solvation entropy Ts_{ex} are found to be less negative than the corresponding experimental values. For pure water at 298 K we obtain $h_{ex} = -7.7$ kJ mol^{-1} (Expt.: $h_{ex} = -10.9$ kJ mol^{-1}) and for the entropy we get $Ts_{ex} = -17.2$ kJ mol^{-1} (Expt.: $Ts_{ex} = -19.3$ kJ mol^{-1}). Note that the larger μ_{ex} of 9.5 kJ mol^{-1} (Expt.: $\mu_{ex} = 8.4$ kJ mol^{-1}) is a consequence of an overemphasized entropy effect, or an underestimation of the solvation enthalpy, or a mixture of both effects simultaneously. The systematic underestimation of the solvation enthalpy seems to be in line with the polarizability arguments raised by Dyer et al.[50] The solute polarizability lowers the excess chemical potential by increasing the magnitude of the solvation enthalpy, and, due to its temperature insensitivity, would affect the temperature dependence of μ_{ex} to a smaller degree. As discussed in ref. [28], the polarizability would therefore only moderately lower the solvation entropy.

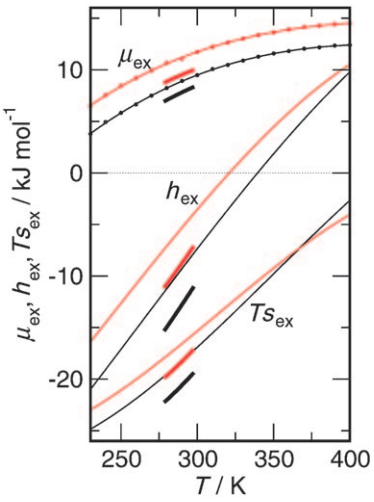

Figure 1. Excess chemical potential (or solvation free energy) μ_{ex}, solvation enthalpy h_{ex} and solvation entropy Ts_{ex} of methane in water and aqueous salt solution as a function of temperature. The short thick lines represent experimental data for methane in pure water (——) and in 2 molar NaCl solution (- - - -).[5] Thin black and red lines are from our MD simulations, describing solvation in pure water, and a 3.85 mol% ≈ 2 molar NaCl aqueous solution, respectively. The symbols indicate solvation free energy data directly obtained from the MD simulation (as given in Table 2), whereas the thin lines correspond to a third order polynomial fit of the MD data.[46]

Recently we have demonstrated that the solvation of small apolar particles in water is very sensitive to the anomalous thermal expansivity behavior of water, and the associated changes in the water structure.[28] By comparing several water models, we observed that models, which are better in agreement with experimental data in terms of structure and thermal expansivity, also exhibit solvation entropies for noble gases and methane closer to the experimental values.[28,47] This is in agreement with what we observe here. Comparing data obtained for the TIP4P-Ew model (which has been optimized to account for water's anomalous properties[30]) with the data for the water models discussed in ref. [28] (SPC, SPCE, TIP3P, TIP4P, TIP5P), we would like to emphasize that the solvation entropy of methane obtained here is closer to the experimental data than the data reported previously.

Comparing the solvation of methane in pure water and a 3.85 mol% $\approx$ 2 molar NaCl solution, we denote an increase of the excess chemical potential $\Delta\mu_{ex} = \mu_{ex(salt\,solution)} - \mu_{ex(water)}$ at 298 K of $+2.25\,kJ\,mol^{-1}$, compared to the $+1.6\,kJ\,mol^{-1}$ observed experimentally. The solvation free energy increase, calculated here for the TIP4P-Ew water model, is very close to the increase of $+2.3\,kJ\,mol^{-1}$ reported by Athawale et al.[21] for a 2 molar salt solution using the SPCE water model.[51] The solvation enthalpy change of $\Delta h_{ex} = +3.8\,kJ\,mol^{-1}$ almost matches the experimental value of $+3.9\,kJ\,mol^{-1}$ and does also not differ strongly from the value found for the SPCE model of $+4.1\,kJ\,mol^{-1}$.[21] Given the larger enthalpic than entropic effect due to the presence of salt at 298 K and following the arguments given by Athawale,[21] our TIP4P-Ew model based simulations clearly also support the view of the salt effect to be "enthalpic" in nature. Considering the whole temperature interval from 230 K to 400 K, the enthalpic effect is found to almost always overcompensate the corresponding entropic contribution in the sense that $\Delta h_{ex} > -\Delta(Ts_{ex})$. At low temperatures h_{ex} is strongly dominating with $\Delta h_{ex} + \Delta(Ts_{ex}) > 5.3\,kJ\,mol^{-1}$ below 300 K. However, with increasing temperature this enthalpic dominance is diminishing, so that at around $T \approx 390$ K enthalpic and entropic contributions are equal of size $\Delta h_{ex} \approx -\Delta(Ts_{ex})$, and the salt effect on the solvation process above this temperature turns over to become "entropic" in nature.

Having traced the temperature dependence of the hydrophobic solvation over a rather broad temperature interval, the fitted data allows us also to reliably determine the second derivative of the solvation free energy: the solvation heat capacity $c_{p,ex}$. For 298 K we find a solvation heat capacity of $192 \pm 10\,J\,K^{-1}\,mol^{-1}$, compared to the $228\,J\,K^{-1}\,mol^{-1}$ according to the data set of Ben-Naim,[5] and the $234\,J\,K^{-1}\,mol^{-1}$ according to Rettich et al.[52] when transforming their data on a number density scale (see ref. [28] for a discussion of this issue). The experimental data of ref. [5] for 298 K indicates that in a 2 molar salt solution, the heat capacity of solvation for methane is lowered to $214\,J\,K^{-1}\,mol^{-1}$. A similar trend is observed also in our computer simulation, where a decrease to $c_{p,ex} = 174 \pm 10\,J\,K^{-1}\,mol^{-1}$ is found at 298 K. Thus, the qualitative change of the thermodynamic solvation properties (free energy, entropy, and enthalpy) as illustrated in Figure 1, with a notable decreasing slope of Ts_{ex} and h_{ex} upon addition of salt, seems to be a quite realistic scenario. An interesting feature of the thermodynamic solvation properties is directly related to the lower solvation heat capacity due to the presence of salt: the solvation entropies of methane dissolved in pure water and in aqueous salt solutions might cross each other at a certain temperature. This is indeed observed in Figure 1 at a temperature of about 367 K, and is finally leading to the crossover from an "enthalpic" to an "entropic" solvation effect for methane at about 390 K, discussed in the previous paragraph.

To summarize, since the salt effect on the solvation heat capacity is essentially well captured by the employed water/salt/methane potential model, the simulations are providing a semi-quantitative description of the salt influence on the solvation thermodynamics up to the second derivative of the free energy with respect to temperature.

2.2. On the Importance of Density Effects

Figure 2a shows the salt dependent contribution to the excess chemical potential $\Delta\mu_{ex} = \mu_{ex(salt\ solution)} - \mu_{ex(water)}$ of methane in an aqueous salt solution for all simulated temperatures and

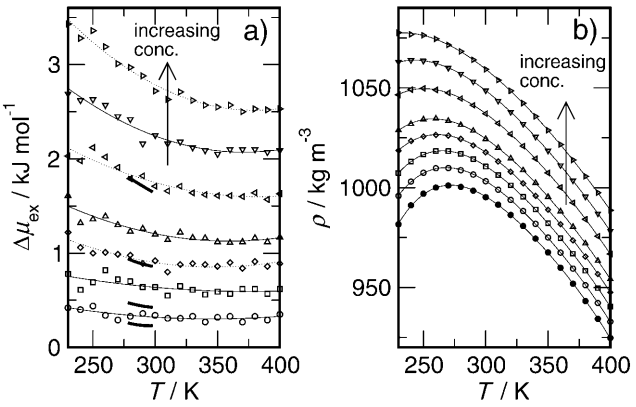

Figure 2. a) Excess chemical potential difference $\Delta\mu_{ex} = \mu_{ex(salt\ solution)} - \mu_{ex(water)}$ between methane dissolved in aqueous salt solution and in pure water. Symbols: data obtained from the MD-simulations corresponding to 0.49, 0.99, 1.48, 1.96 2.91, 3.85, and 4.76 mol% composition, respectively. The arrow indicates increasing salt concentration. The thick heavy lines indicate experimental data of Ben-Naim and Yaacobi[5] for 0.25, 0.5, 1.0, and 2.0 mol l^{-1}, respectively. b) Density of the aqueous salt solutions as obtained from the MD simulations. The filled circles indicate pure water data.

compositions. Note that at supercooled conditions the $\Delta\mu_{ex}$ exhibit a significantly larger response due to the addition of salt, than at higher temperatures, where the calculated $\Delta\mu_{ex}$ almost seem to approach constant values. This behavior is, however, a manifestation of the observed lowering of solvation entropies and heat capacities in salt solutions, as discussed in the previous section. Based on computer simulation studies we have previously argued that volume effects have a strong influence on the solvation free energy of hydrophobic particles.[28] These observations were in accord with the predictions of the information theory model of hydrophobic hydration[53,54] and have been recently further substantiated by the work of Ben-Amotz

and Widom.[55,56] To obtain temperature dependent solvation quantities, such as entropies and enthalpies, close to the experimental data, it is therefore for example, desirable that the employed water model correctly accounts for the anomalous temperature dependence of waters density. Docherty et al.[26] calculated recently a related quantity called "packing fraction" from simulations of aqueous salt solutions. They showed that this quantity scales well with the excess chemical potential of methane with varying salt concentration. It is therefore not unlikely to expect that salt-induced density effects, as well as their temperature dependence, are similarly important for the solubility of methane in aqueous salt solutions. Figure 2b shows the densities obtained from the MD simulations. Most notable is a shift of the temperature of maximum density (with a $T_{md}=271$ K for pure TIP4P-Ew) which has been estimated here to be about -6.7 ± 1.0 K mol%$^{-1}$ (see also ref. [27]), being close to the experimental value of -7.9 K mol%$^{-1}$ (determined over the whole concentration range given in ref. [57]). Note, however, that the absolute change in density due to the addition of salt, is significantly underestimated by our MD simulations with about 13.1 kg m^{-3} mol%$^{-1}$, compared to the 21 kg m^{-3} mol%$^{-1}$ observed experimentally at 298 K.[57]

From computer simulations of water, S. Garde et al. have derived an information theory (IT) model,[53,54] proposing simple analytic expressions for the hydrophobic hydration as a function of temperature and density. The leading term in the IT model strongly suggests a quadratic relation between the excess chemical potential and the solvent number density ρ' according to $\mu_{ex}/k\approx\rho'^2Tv^2/2\sigma_n^2$,[54] where v denotes the volume of a hydrophobic hard sphere particle, while $\sigma_n^2=\langle n^2\rangle-\langle n\rangle^2$ indicates the variance of the number of water molecules in a sphere of volume v. Figure 3 indicates a temperature dependence as suggested by the IT model, assuming the term $a=v^2/2\sigma_n^2$ to be constant (and the same for all concentration shown here) and shifting by a constant b offset to account for attractive interactions. As an approximation, we employ here the mass density ρ of the aqueous salt solutions. In line with recent results on the effect of pressure and temperature on the solubility of small apolar particles in a TIP5P-E water model solvent,[29] the simple relation describes the behavior of the solvation of methane in the salt solutions quite successfully. For pure TIP4P-Ew water the prediction is almost quantitative, whereas with increasing amount of salt both the behavior with respect to salt concentration and with respect to temperature becomes less accurate, particularly at very high temperatures. However, the relation is well-behaving in the sense that it predicts a lowering of the solvation heat capacity with increasing salt concentration, as well as an increase of Ts_{ex} for low temperatures, in accordance with the MD data. The predicted temperature, where methane exhibits equal solvation entropies in salt solution and in pure water of about 300 K, however, is significantly too low, compared to the value of 367 K found in Figure 1.

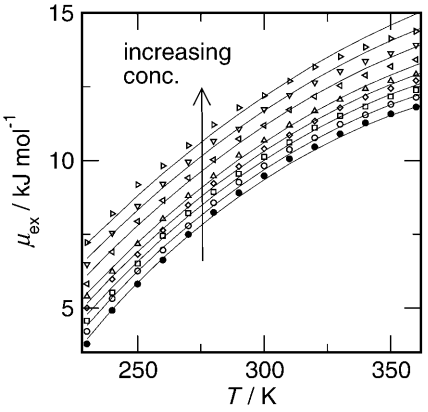

Figure 3. Excess chemical potential μ_{ex} of methane in water and aqueous salt solutions. Symbols: data obtained directly from the MD simulations. Filled circles: pure water. Open Symbols: aqueous salt solutions as given in Figure 2a. Full lines: predictions with $\mu_{ex}=a\rho^2T+b$ with $a=7.15\times10^{-2}$ kJ mol^{-1} K^{-1} cm^6 g^{-2} and $b=-11.9$ kJ mol^{-1}.

Finally, we would like to point at an observation which perhaps deserves further attention. The simple scaling relation based on the IT model seems to describe the solvation data quite satisfactorily. Hence, one would expect a larger $\Delta_t\mu_{ex}$ for the experimental data than it is observed for our MD simulations, as the experimental density changes more strongly upon adding salt. However, the opposite is true. The experimental value of 1.6 kJ mol^{-1} for a 2 molar salt solution is actually smaller than the 2.25 kJ mol^{-1} calculated from MD. A possible explanation might be that that a potentially larger "repulsive" hard sphere component of $\Delta_t\mu_{ex}$, as predicted by the IT model due to more strongly density effect, might be effectively counterbalanced by an enhanced "attractive" interaction promoted by solute polarization effects due to the ions (which were neglected in the present calculations).

2.3. Local Versus Global Salt Effects

Here we determine to which degree the described salt effects on the solubility of methane are either caused by "local" effects, associated with direct or solvent separated contact of methane with the ions, or by "global" effects induced by structural alterations of the solvent bulk phase. Therefore we propose a partitioning of the volume of the entire simulation cell into "shell" and "bulk" regions, as graphically illustrated in Figure 4. The "shell" partitioning includes first and second hydration shells of the ions, described in Figure 4, and is constructed in such a way that the "shell" and "bulk" sub volumes add up to the volume of the entire simulation cell.[58] During the computation of the excess chemical potential we have monitored whether the Monte Carlo insertion was probing either the "shell" or the "bulk" sub-volume, and could thus determine the associated components to the excess chemical potential $\mu_{ex,bulk/shell}=-kT\ln\langle\exp(-\beta\Phi(\vec{r}))\rangle_{bulk/shell}$. Figure 5a shows the relative changes of the solvation free energy in a 3.85 mol%$\approx$2 mol l^{-1} NaCl solution for each of the sub-volumes. Here the bulk-volume contribution (bulk volume fraction) here about 50% for a 2 mol l^{-1} NaCl, slightly varying with temperature. Note that the compact packing of water in the hydration shells of the ions significantly elevates the chemical potential of methane. But also for the "bulk" part we find that methane's chemical potential is significantly larger than in

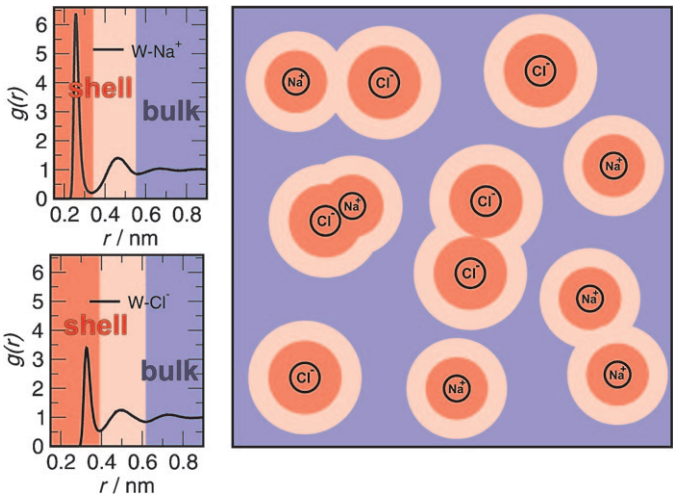

Figure 4. Cartoon representation of the structure of an aqueous salt solution. The first and second minima of the ion-water pair correlation functions determine the radii of the first and second hydration shells, here indicated by dark and light red coloring. The red shaded region[58] is considered as "shell", whereas the blue shaded region will be referred to as "bulk". The total amount of the "shell" region (which is directly influenced by the ions) depends strongly on the tendency of the ions to form like and unlike solvent separated and close contact pairs.

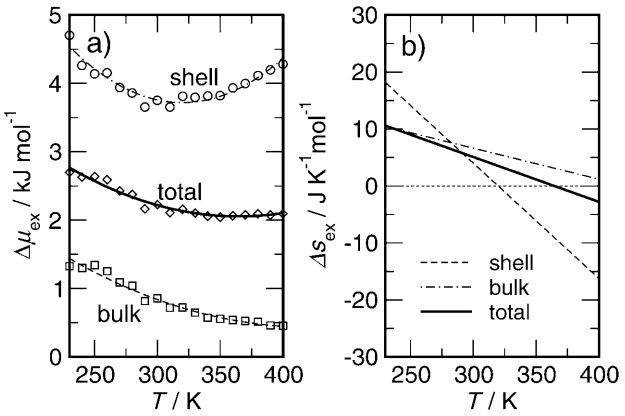

Figure 5. a) Excess chemical potential difference $\Delta\mu_{ex}=\mu_{ex(salt\ solution)}-\mu_{ex(water)}$ of methane dissolved in aqueous salt solution (here 3.85 mol% ≈ 2 mol l^{-1}) and in pure water. We distinguish between ion hydration-shell ("shell") and water-bulk ("bulk") volumes according to ref. [58]. The solid lines indicate second order polynomial fits to the data with respect to the temperature. b) Solvation entropy difference $\Delta s_{ex}=s_{ex(salt\ solution)}-s_{ex(water)}$ between methane dissolved in aqueous salt solution and in pure water. The lines are obtained as temperature derivative of the fitted polynomial shown in Figure 5a.

pure water. Note that also the temperature dependence of the solvation free energy of methane behaves significantly different in "bulk" and "shell". In Figure 5b we quantify the temperature effect by calculating the corresponding solvation entropies. Note that the obtained entropies for the sub-volumes are subject to an error of about $\pm 5\ J K^{-1} mol^{-1}$, therefore the lines for the sub-volumes do not properly add up to average "total" values. However, the trends are clear. At sufficiently low temperatures, "bulk" and "shell" regions contribute both to the observed increase of the solvation entropy. The "shell" contribution, however, exhibits a markedly stronger temperature dependence, leading finally to a significantly pronounced negative entropy contribution at high temperatures. The negative slope of the entropy curves, depicted in Figure 5b, suggests that the negative solvation heat capacity contribution due to the presence of salt has to be attributed to both, bulk and shell region. The contribution of the ion hydration shells is, however, clearly dominating.

Figure 6 illustrates how the chemical potentials obtained for the "bulk" and "shell" regions contribute to the increasing solvation free energy. The bulk-volume contribution (bulk volume

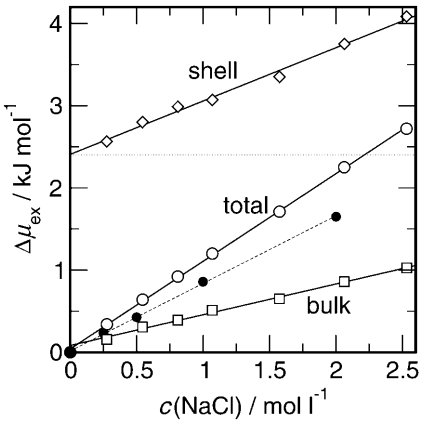

Figure 6. Excess chemical potential difference $\Delta\mu_{ex}=\mu_{ex(salt\ solution)}-\mu_{ex(water)}$ for methane dissolved in aqueous salt solution and in pure water at $T=300$ K. In addition we distinguish between contributions coming from ion hydration-shell and water-bulk sub volumes.[58] The filled symbols indicate the experimental data of Ben-Naim and Yaacobi for $T=298$ K.[5]

fraction) reduces up to 35% for the 2.5 mol l^{-1} NaCl solution. As a reference we have also given the experimental data of Ben-Naim and Yaacobi,[5] once again indicating the overestimation of the salt contribution to the ("total") solvation free energy. Note that both "bulk" and "shell" contributions increase with rising salt concentration. Both are only slightly differing in slope. This is suggesting that with an increasing salt concentration both bulk and shell apparently respond in a very similarly way, perhaps in terms of a tighter packing of the water. This might be due to a "global" compression of the entire salt solution caused by electrostriction effects.[12,27] In addition, the "shell" data exhibits a significant offset due to the specific water structure in the ion hydration shells and the particular interaction of methane with the ions. The observed large increase of the total solvation free energy is apparently composed of the individual soft responses of the "bulk" and "shell" contributions, and the simple fact that shell-contribution becomes increasingly dominant as the concentration rises. As a consequence, the observed resulting total slope of $\Delta\mu_{ex}$ vs concentration is tightly related to the ratio of "shell" and "bulk" water. This ratio, in addition, is significantly affected by the tendency of the ions to form contact or solvent separated ion pairs. We would like to point out that this mechanism has some resemblance to what has been suggested by K. D. Collins.[16]

In the previous section we have observed an enhanced response of $\Delta\mu_{ex}$ upon addition of salt at low temperatures (see

Figure 2a). Figure 7 now illustrates the different responses at low and high temperatures for "bulk" and "shell". Note that the enhanced response is the consequence of two effects. First

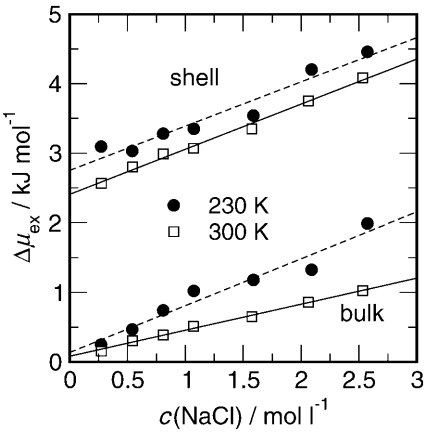

Figure 7. Excess chemical potential difference $\Delta\mu_{ex}=\mu_{ex(salt\ solution)}-\mu_{ex(water)}$ for methane dissolved in aqueous salt solution and in pure water at $T=230$ K and $T=300$ K. We distinguish between contributions from ion hydration-shell "shell" and water-bulk "bulk" sub volumes.[58]

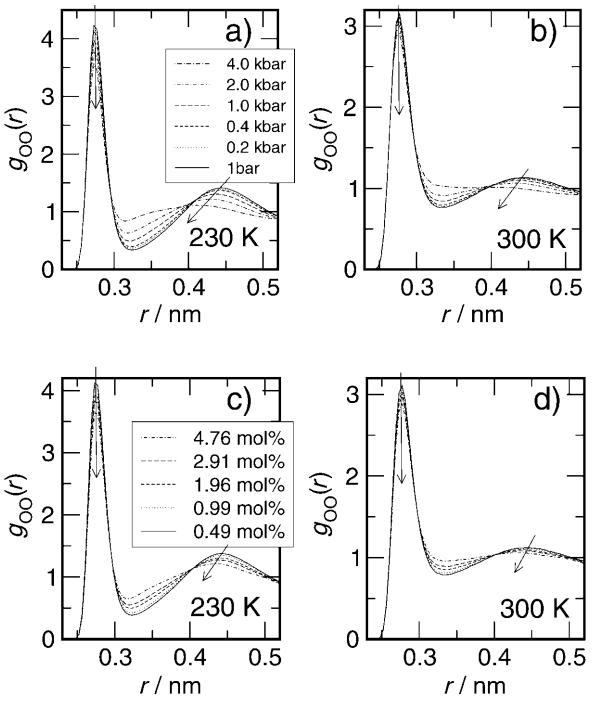

Figure 8. Oxygen-oxygen radial distribution functions for pure TIP4P-Ew water at different pressures (a,b) and for aqueous salt (NaCl) solutions at various concentrations. Pair correlations for water under pressure were calculated from simulation data reported in ref. [27]. Two temperatures are shown: a,c) $T=230$ K; b,d) $T=300$ K. Arrows indicate the position and shift of the first and second maximum as pressure or salt concentration increases.

of all, the bulk phase alone responses more strongly at low temperatures. This seems to be in agreement with the enhanced density-response at low temperatures, which is intimately related with shift of the temperature of maximum density towards lower temperatures with increasing salt concentration (see Figure 2b). Secondly, the excess chemical potential exhibits a slightly increased offset in the shell region, apparently related to a better ordering of the water molecules in the ion solvation shell at low temperatures.

To summarize, the chemical potential of methane is found to be systematically affected by the presence of salt in both "shell" and "bulk" sub volumes, emphasizing the importance of the global volume contraction due to electrostriction effects.

2.4. Structural Considerations

First we discuss the changes in water structure caused by the addition of salt. The water-water site-site radial distribution functions (RDFs) $g_{OO}(r)$, $g_{HO}(r)$ and $g_{HH}(r)$ were calculated as a function of temperature and salt concentration. The oxygen–oxygen pair correlation functions $g_{OO}(r)$, given in Figure 8, have been recently suggested to be the most sensitive RDF to detailed changes of the water structure.[59] Figure 8 focuses on the observed salt effect on the location and height of the first two maxima. This is compared to the behavior observed for enhanced hydrostatic pressure, calculated previously.[27] The water–water correlations change significantly with increasing salt concentration. In particular we see by adding salt that the first peak in the RDF shrinks, and the second peak, which is traditionally regarded as the signature of tetrahedral bonding in water, moves markedly inwards.

For pure water it has been shown by the experiments of Soper and Ricci, that the second peak of $g_{OO}(r)$ moves to shorter distances upon application of an external pressure.[60] This feature is also observed here for the TIP4P-Ew model[27] at low and high temperatures, as shown in Figures 8a and b. As suggested by Soper and Ricci, this is indicative of a distorted, but not necessarily broken, hydrogen bond network, and eventually causes the collapse of the second neighboring shell into the first one[60]at very high pressures. In addition, the second maximum of the RDFs is found to be more pronounced at 230 K compared to 300 K, in line with the observation of a more tetrahedrally ordered water structure at lower temperatures.[61]

A similar behavior is found with increasing salt concentration at both temperatures, as indicated by Figures 8c,d. The inward shift of the second peak at low, but as well at high temperatures, suggest that the water structure is modified by the presence of ions in a similar fashion as due to pressure. Lebermann and Soper[62] used neutron diffraction to compare the effects of pressure and high salt concentrations on the hydrogen-bonded network of water. They found that the ions induce a change in structure, equivalent to the application of high pressures, and that the magnitude of the effect is ion-specific.[62] Similar effects have been reported by Botti et al.[63,64] who studied the solvation shell of H^+ and OH^- ions in water. Mancinelli et al. could show that the structural perturbation due to monovalent ions (in aqueous solutions of NaCl and KCl) exists also outside the first hydration shell of the ions.[59] Moreover, in line with observations on the effect of salt on the phase behavior of metastable water by MD simulations of Corradini et al.,[65] Holzmann et al.[27] found that the ions seem to

prevent water from transforming into a highly tetrahedrally ordered liquid at deeply supercooled conditions.

The overall structural influence of the ions is nicely demonstrated by the changing site–site pair correlation functions with $\Delta g_{XY}(r) = g_{XY}(r)_{\text{salt solution}} - g_{XY}(r)_{\text{pure water}}$. All $\Delta g_{XY}(r)$ are shown in Figure 9 for 230 K and 300 K, respectively. $\Delta g_{OH}(r)$ indicates that the addition of salt leads to a significant decrease in the hydrogen bonding peak at 0.185 nm. This effect is significantly more pronounced at 230 K. The more ordered tetrahedral network at lower temperatures is eventually more strongly affected by addition of salt. The broader negative peak of $\Delta g_{OH}(r)$ at about 0.5 nm is related to the decrease in the second peak of $g_{OO}(r)$ in Figure 8, indicating distortion and diminution of the tetrahedral coordination of the water molecules. Again this effect is found to be more pronounced in the supercooled region. The broad peak around 0.31 nm of $\Delta g_{HH}(r)$ suggests an increase in the nearest neighbor $g_{HH}(r)$ peak (Figure 9c). Overall, our calculated $\Delta g_{HH}(r)$ is in good agreement with the data obtained by Leberman and Soper from neutron diffraction of a 4 mol l^{-1} sodium chloride solution.[62] They report a negative region near radius $r = 0.2$ nm, a positive region near $r = 0.3$ nm, and a broad negative region around 0.45 nm, in accord with our values of 0.23 nm, 3.1 nm, and 0.5 nm, respectively. Overall, the structural changes caused by the addition of salt appear to be very similar to the change for pure water due to increasing pressure.

In the final part of this section we would like to discuss the structure of the solution in the vicinity of the methane particle. The methane water, and the methane ion radial pair distribution functions for different salt concentrations, obtained by the Widom particle insertion technique, are shown in Figure 10. We would like to point out that the radial distribution functions shown here have, in general, great similarity with the RDFs given by Athawale et al.[21] and others.[66,24] The tight packing of water around the sodium cation largely prevents a direct contact between sodium and methane, as the absence of a pronounced first peak in Figure 10a suggests. The somewhat more loose water packing around the chloride ion, however, permits a close encounter configuration, but there is no particularly enhanced methane-ion aggregation. The large positive offset calculated for the "shell " contribution of $\Delta\mu_{ex}$ discussed earlier (see Figure 6), hence has to be attributed largely to the repulsiveness of the sodium cation. The observation of a slightly increasing peak height for all RDFs with increasing salt concentration is in accordance with previous findings.[21] Comparing the effect of salt concentration, we observe an increase of about 0.1 to 0.15 for all pair correlation functions, water and ions, as we increase the salt concentration from 0.99 mol% to 4.76 mol%. Since none of the possible (water,anion,cation)-methane contacts is apparently strongly preferred, the salt might be considered behaving "neutrally". This observation seems to be in good qualitative agreement with the observation of a very similar response of the excess chemical potential $\Delta\mu_{ex}$ for "bulk" and "shell" regions with increasing salt concentration, as shown in Figure 6.

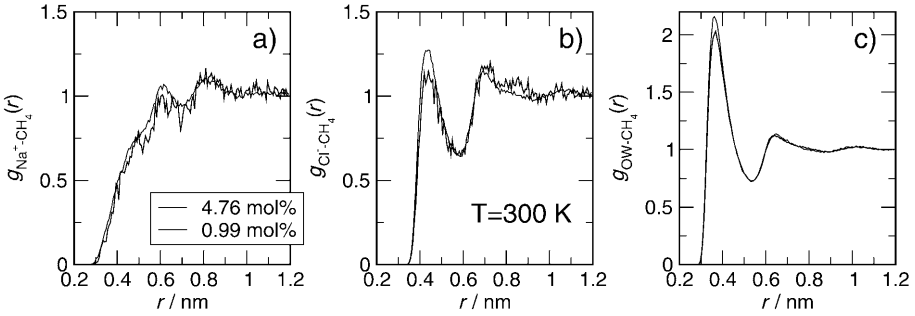

Figure 10. Methane-ion and methane-water oxygen radial pair distribution functions for the aqueous salt solution with 0.99 mol% NaCl and 4.76 mol% NaCl, obtained at $T = 300$ K.

3. Conclusions

We have performed MD simulations of aqueous NaCl solutions using the TIP4P-Ew water model,[30] covering broad temperature and concentration ranges, extending deeply into the supercooled region. We have studied the effect of temperature and salt concentration on the solvation of methane at infinite dilution. The salt effect on methane's solvation free energy, solvation enthalpy and entropy, as well as their temperature dependence is found to be semi-quantitatively in accordance with the data of Ben-Naim and Yaacobi.[5] The salt contribution to the solvation free energy is found to be "enthalpic" at low temperatures, but becomes "entropic" above 390 K. To distinguish the influence of local (in close proximity to ions) and global effects, we partition the salt solutions into ion influenced hydration shell regions and bulk water. The chemical potential of methane is found to be systematically affected by the presence of salt in both sub volumes, emphasizing the importance of the global volume contraction due to

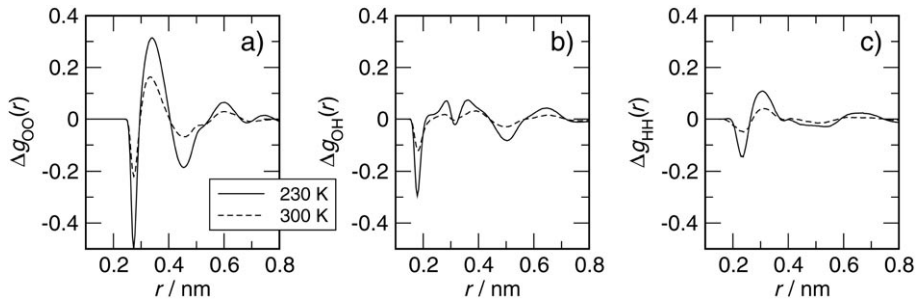

Figure 9. Water-water site-site difference radial pair distribution functions $\Delta g_{XY}(r) = g_{XY}(r)$[salt-solution] $- g_{XY}(r)$[water] for an aqueous TIP4P-Ew salt solution with 3.85 mol% NaCl at $T = 230$ K and $T = 300$ K.

electrostriction effects. The chemical potential of methane increases quite similarly in "bulk" and "shell" with rising salt concentration. Since the salt effect on the methane-water and methane-ion pair correlation functions is also found to be very similar, the simulated NaCl behaves rather "neutral" with respect to the solvation of methane. The influence of salt is accompanied with systematic alterations of the water structure, similar to water under pressure. The observed electrostriction effects are found to become increasingly pronounced under cold (supercooled) conditions. We find that the influence of temperature and salt induced global density changes on the solvation properties of methane is well recovered by a simple scaling relation based on predictions of the information theory model of Garde et al.[53]

Acknowledgements

This work was supported by the Deutsche Forschungsgemeinschaft (Forschergruppe 436) and the "Pact for Research and Innovation of the Federal Ministry of Education and Research/Leibniz Science Association".

Keywords: electrostriction effects · methane · molecular dynamics · solvation dynamics · thermodynamics

[1] C. Tanford, *The Hydrophobic Effect: Formation of Micelles and Biological Membranes, 2nd ed.*, Wiley, New York, **1980**.
[2] A. Ben-Naim, *Hydrophobic Interactions*, Plenum, New York, **1980**.
[3] N. T. Southall, K. A. Dill, A. D. J. Haymet, *J. Phys. Chem. B* **2002**, *106*, 521–533.
[4] B. Widom, P. Bhimalapuram, K. Koga, *Phys. Chem. Chem. Phys.* **2003**, *5*, 3085–3093.
[5] A. Ben-Naim, M. Yaacobi, *J. Phys. Chem.* **1974**, *78*, 170–175.
[6] W. L. Masterton, D. Bolocofsky, T. P. Lee, *J. Phys. Chem.* **1971**, *75*, 2809–2815.
[7] M. Kinoshita, F. Hirata, *J. Chem. Phys.* **1997**, *106*, 5202–5215.
[8] W. Kunz, P. L. Nostro, B. W. Ninham, *Curr. Opin. Colloid Interface Sci.* **2004**, *9*, 1–18.
[9] H. S. Frank, F. Franks, *J. Chem. Phys.* **1968**, *48*, 4746–4757.
[10] F. Franks, *Biophys. J.* **2002**, *96*, 117–127.
[11] O. Y. Samoilov, *Structure of Aqueous Electrolyte Solutions and the Hydration of Ions*, Consultants Bureau, New York, **1965**.
[12] B. Hribar, N. T. Southall, V. Vlachy, K. A. Dill, *J. Am. Chem. Soc.* **2002**, *124*, 12302–12311.
[13] K. D. Collins, M. W. Washabaugh, *Q. Rev. Biophys.* **1985**, *18*, 323–422.
[14] R. L. Baldwin, *Biophys. J.* **1996**, *71*, 2056–2063.
[15] K. A. Dill, T. M. Truskett, V. Vlachy, B. Hribar-Lee, *Annu. Rev. Biophys. Biomol. Struct.* **2005**, *34*, 173–199.
[16] K. D. Collins, *Biophys. J.* **1997**, *72*, 65–76.
[17] A. S. Thomas, E. H. Elcock, *J. Am. Chem. Soc.* **2007**, *129*, 14887–14898.
[18] S. N. Timasheff, *Adv. Protein Chem.* **1998**, *51*, 355–432.
[19] T. Arakawa, S. N. Timasheff, *Biochemistry* **1982**, *21*, 6545–6552.
[20] R. Zangi, M. Hagen, B. J. Berne, *J. Am. Chem. Soc.* **2007**, *129*, 4678–4686.
[21] M. V. Athawale, S. Sarupria, S. Garde, *J. Phys. Chem. B* **2008**, *112*, 5661–5670.
[22] P. E. Smith, *J. Phys. Chem. B* **1999**, *103*, 525–534.
[23] T. Ghosh, A. E. García, S. Garde, *J. Phys. Chem. B* **2003**, *107*, 612–617.
[24] T. Ghosh, A. Kalra, S. Garde, *J. Phys. Chem. B* **2005**, *109*, 642–651.
[25] H. Docherty, A. Galindo, C. Vega, E. Sanz, *J. Chem. Phys.* **2006**, *125*, 074510.
[26] H. Docherty, A. Galindo, E. Sanz, C. Vega, *J. Phys. Chem. B* **2007**, *111*, 8993–9000.
[27] J. Holzmann, R. Ludwig, D. Paschek, A. Geiger, *Angew. Chem.* **2007**, *119*, 9065–9069; *Angew. Chem. Int. Ed.* **2007**, *46*, 8907–8911.
[28] D. Paschek, *J. Chem. Phys.* **2004**, *120*, 6674–6690.
[29] D. Paschek, *Phys. Rev. Lett.* **2005**, *94*, 217802.
[30] H. W. Horn, W. C. Swope, J. W. Pitera, J. D. Madura, T. J. Dick, G. L. Hura, T. Head-Gordon, *J. Chem. Phys.* **2004**, *120*, 9665–9678.
[31] K. Heinzinger in *Computer Modelling of Fluids Polymers and Solids, NATO ASI Series, Vol. C293* (Eds.: C. R. A. Catlow, S. C. Parker, M. P. Allen), Kluwer Dordrecht, **1990**, pp. 357–369.
[32] U. Essmann, L. Perera, M. L. Berkowitz, T. A. Darden, H. Lee, L. G. Pedersen, *J. Chem. Phys.* **1995**, *103*, 8577–8593.
[33] S. Miyamoto, P. A. Kollman, *J. Comput. Chem.* **1992**, *13*, 952–962.
[34] E. Lindahl, B. Hess, D. van der Spoel, *J. Mol. Model.* **2001**, *7*, 306–317.
[35] S. Nosé, *Mol. Phys.* **1984**, *52*, 255–268.
[36] W. G. Hoover, *Phys. Rev. A* **1985**, *31*, 1695–1697.
[37] M. Parrinello, A. Rahman, *J. Appl. Phys.* **1981**, *52*, 7182–7190.
[38] S. Nosé, M. L. Klein, *Mol. Phys.* **1983**, *50*, 1055–1076.
[39] B. Widom, *J. Chem. Phys.* **1963**, *39*, 2808–2812.
[40] J. O. Hirschfelder, C. F. Curtiss, R. B. Bird, *Molecular Theory of Gases and Liquids*, Wiley, New York, **1954**.
[41] B. Guillot, Y. Guissani, *J. Chem. Phys.* **1993**, *99*, 8075–8094.
[42] C. H. Bennett, *J. Comput. Phys.* **1976**, *22*, 245–268.
[43] K. S. Shing, K. E. Gubbins, *Mol. Phys.* **1983**, *49*, 1121–1138.
[44] G. L. Deitrick, L. E. Scriven, H. T. Davis, *J. Chem. Phys.* **1989**, *90*, 2370–2385.
[45] G. L. Deitrick, L. E. Scriven, H. Davis, *Mol. Simul.* **1992**, *8*, 239–247.
[46] Fitted excess chemical potential $\mu_{ex}(T)=\mu_0+\mu_1 T+\mu_2 T^2+\mu_3 T^3$ of methane in water and aqueous salt solution. Water: $\mu_0=-4.89\times10^1$ kJ mol^{-1}, $\mu_1=3.76\times10^{-1}$ kJ mol^{-1}K^{-1}, $\mu_2=-7.46\times10^{-4}$ kJ mol^{-1}K^{-2}, $\mu_3=4.74\times10^{-7}$ kJ mol^{-1}K^{-3}. 3.85 mol% NaCl solution: $\mu_0=-4.48\times10^1$ kJ mol^{-1}, $\mu_1=3.76\times10^{-1}$ kJ mol^{-1}K^{-1}, $\mu_2=-7.94\times10^{-4}$ kJ mol^{-1}K^{-2}, $\mu_3=5.61\times10^{-7}$ kJ mol^{-1}K^{-3}.
[47] P. E. Krouskop, J. D. Madura, D. Paschek, A. Krukau, *J. Chem. Phys.* **2006**, *124*, 016102.
[48] S. Shimizu, H. S. Chan, *J. Chem. Phys.* **2000**, *113*, 4683–4700.
[49] D. Paschek, *J. Chem. Phys.* **2004**, *120*, 10605–10617.
[50] P. J. Dyer, H. Docherty, P. T. Cummings, *J. Chem. Phys.* **2008**, *129*, 024508.
[51] H. J. C. Berendsen, J. R. Grigera, T. P. Straatsma, *J. Phys. Chem.* **1987**, *91*, 6269–6271.
[52] T. R. Rettich, Y. Handa, R. Battino, E. Wilhelm, *J. Phys. Chem.* **1981**, *85*, 3230–3237.
[53] S. Garde, G. Hummer, A. E. García, M. E. Paulaitis, L. R. Pratt, *Phys. Rev. Lett.* **1996**, *77*, 4966–4968.
[54] G. Hummer, S. Garde, A. E. García, L. R. Pratt, *Chem. Phys.* **2000**, *258*, 349–370.
[55] D. Ben-Amotz, B. Widom, *J. Phys. Chem. B* **2006**, *110*, 19839–19849.
[56] D. Ben-Amotz, B. Widom, *J. Chem. Phys.* **2007**, *126*, 104502.
[57] *International Critical Tables of Numerical Data, Physics, Chemistry and Technology, Vol. III* (Ed.: E. W. Washburn), Mc Graw Hill, New York, **1928**.
[58] We distinguish between "bulk" and "shell" volume. Around each ion a sphere is drawn with a radius containing essentially the first and second hydration shells of the ions. ($r_{W\text{-}Na} \leq 0.55$ nm and $r_{W\text{-}Cl} \leq 0.62$ nm). The volume enclosed by all of these spheres is labeled "shell". The volume outside these spheres is referenced to as "bulk".
[59] R. Mancinelli, A. Botti, F. Bruni, M. A. Ricci, A. K. Soper, *Phys. Chem. Chem. Phys.* **2007**, *9*, 2959–2967.
[60] A. K. Soper, M. A. Ricci, *Phys. Rev. Lett.* **2000**, *84*, 2881–2884.
[61] D. Paschek, A. Geiger, *J. Phys. Chem. B* **1999**, *103*, 4139–4146.
[62] R. Leberman, A. K. Soper, *Nature* **1995**, *378*, 364–366.
[63] A. Botti, F. Bruni, S. Imberti, M. A. Ricci, A. K. Soper, *J. Mol. Liq.* **2005**, *117*, 77–79.
[64] A. Botti, F. Bruni, S. Imberti, M. A. Ricci, A. K. Soper, *J. Mol. Liq.* **2005**, *117*, 81–84.
[65] D. Corradini, P. Gallo, M. Rovere, *J. Chem. Phys.* **2008**, *128*, 244508.
[66] N. Kalra, N. Tugcu, S. M. Cramer, S. Garde, *J. Phys. Chem. B* **2001**, *105*, 6380–6386.

Received: August 17, 2008
Revised: November 6, 2008
Published online on November 28, 2008

